Geomechanics and Engineering, *Vol. 16, No. 2 (2018) 159-168*
DOI: https://doi.org/10.12989/gae.2018.16.2.159

Clogging theory-based real time grouting management system applicable in soil conditions

Young-Sam Kwon[1a], Jinchun Kim[2b] and In-Mo Lee[*1]

[1]*School of Civil, Environmental and Architectural Engineering, Korea University, 145, Anam-ro, Seongbuk-gu, Seoul, Republic of Korea*
[2]*Korea Institute of Geo Technology Inc., 14 Sagimakgol-ro 45beon-gil, Jungwon-gu, Seongnam-si, Gyeonggi-do, Republic of Korea*

(Received October 27, 2017, Revised March 7, 2018, Accepted May 21, 2018)

Abstract. In this study, a real-time grouting management system based on the clogging theory was established to manage injection procedure in real time. This system is capable of estimating hydraulic permeability with the passage of time as the grout permeates through the ground, and therefore, capable of estimating real time injection distance and flow rate. By adopting the Controlled Injection Pressure (CoIP) model, it was feasible to predict the grout permeation status with the elapse of time by consecutively updating the hydraulic gradient and flow rate estimated from a clogging-induced alteration of pore volume. Moreover, a method to estimate the volume of the fractured gap according to the reduction in injection pressure was proposed. The validity of the proposed system was successfully established by comparing the estimated values with the measured field data.

Keywords: real time grouting management system; permeation grouting; clogging theory

1. Introduction

Owing to the advancement in technology and increasing globalization, human migration and transportation of goods are becoming more and more popular. Accordingly, the necessity for the construction of underwater tunnels, a means of transportation by which people and goods can be shifted from one continent to an island and/or another continent without being affected by weather, is increasing. In addition, flood/drought damage caused by rapid climate change is increasing and demand of dam or reservoir is steadily increasing to prevent these damages. One of the most fundamental technologies required for the safe construction of above cases is the grouting method. Safe construction is feasible only when the permeability coefficient is adequately controlled during dam/reservoir construction and/or during tunnel driving, etc. Proper grouting regulation is essential; improper regulation of grouting pressure is likely to cause a risky situation wherein hydraulic fracturing occurs in the ground.

Among grouting methods, cement-based grouting is the most widely used worldwide. Recent advances in computer technology has resulted in continuous advancement of injection theory and equipment (Taylor and Choquet 2012) and development of advanced grouting management method (Do *et al.* 2012). For example, grouting work can at present be monitored in real time using computers (Fan *et al.* 2016). Another example is where a grout injection control scheme has been studied in which the grout is injected into a rock bed using the characteristics of a Bingham fluid (Kobayashi *et al.* 2008).

However, according to a recent study, a fluid such as cement milk behaves as a Newtonian fluid when the water-to-cement (w/c) ratio is high (i.e., w/c $\geq$ 1.25) and as a Bingham fluid or a power-law fluid when the ratio is low (i.e., w/c < 1.25) (Yang, *et al.* 2011). To achieve permeation grouting through soils, a high value of w/c ratio, for e.g., w/c > 1.5, is generally selected in practice. Then, the grout material behaves as a Newtonian fluid; recent study verified that the clogging phenomenon, rather than the yield stress, fulfills a key function in the regulation of penetration characteristics in the case of permeation grouting with a Newtonian fluid (Axelsson *et al.* 2009). Accordingly, in this study, a real time grouting management system that applies to soils using a Newtonian fluid was established on the basis of clogging theory. It is feasible to predict the flow rate and injection pressure in real time with the developed system; moreover, a method to predict and manage fracturing injection that is likely to occur unexpectedly during permeation grouting, was presented. We would like to emphasize again that this study focused on cement milk grouting which behaves as a Newtonian fluid.

2. Real time grouting management system

2.1 Overview of extant method

Kim *et al.* (2009) proposed a step-wise numerical calculation (SWNC) method for analyzing permeation grouting of soils on the basis of clogging theory (see Fig. 1). Using the SWNC model, the time required to inject

*Corresponding author, Professor,
E-mail: inmolee@korea.ac.kr
[a]Ph.D. Candidate,
E-mail: bchkasu@korea.ac.kr
[b]President,
E-mail: kig-2000@hanmail.net

ISSN: 2005-307X (Print), 2092-6219 (Online)

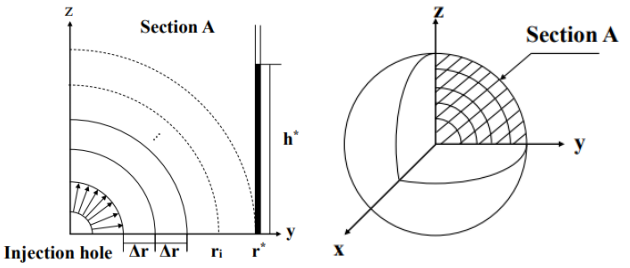

Fig. 1 Analytical model for permeation grouting with variable Δt_i and constant Δr (Kim *et al.* 2009)

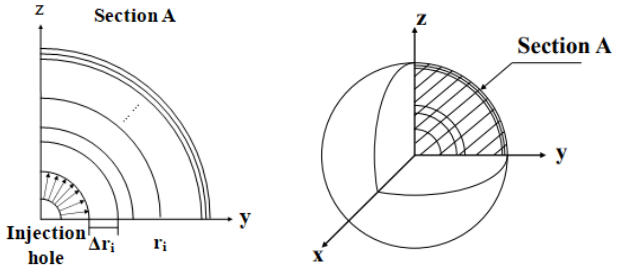

Fig. 2 Modified permeation grouting model with variable Δr_i and constant Δt

grout till unit penetration distance (Δr) can be obtained using updated value of the porosity of the ground, which varies owing to the clogging phenomenon of the grout, and that of the permeability coefficient.

Grout material is assumed to penetrate into the ground spherically as illustrated in Fig. 1, and the penetration model is described using spherical shells of width Δr. In this condition, the injection volume required for penetration up to between r_i and r_{i-1} is expressed by Eq. (1)

$$q_i = \frac{4}{3}\pi[{r_i}^3 - {r_{i-1}}^3] \cdot \frac{n}{\Delta t_i} \tag{1}$$

where n is the porosity of the ground, and Δt_i is the time required for the grout particles to advance from r_{i-1} to r_i. It is known that if a grout material shows the Newtonian behavior, the assumption of Darcy's law and steady-state laminar flow is valid (Raffle and Greenwood, 1961). Based on Darcy's law, the injection volume can also be expressed, in the following form

$$q_i = K_g \cdot i \cdot \bar{A}_i \tag{2}$$

where K_g is the permeability coefficient of the grout penetrating into the ground pores, i is the hydraulic gradient, and $\bar{A}_i$ is the average cross-sectional area between r_{i-1} and r_i. If Δr is sufficiently small, the average cross-sectional area $\bar{A}_i$ can be expressed as follows

$$\bar{A}_i = \frac{4\pi}{3\Delta r}({r_i}^3 - {r_{i-1}}^3) \tag{3}$$

By combining Eqs. (1)-(3), Δt_i can be expressed as follows

$$\Delta t_i = \frac{\Delta r \cdot n}{\gamma_g \cdot K_{int} \cdot i}\mu_g(t_{i-1}) \tag{4}$$

where K_{int} is the intrinsic permeability coefficient of the ground; γ_g is the unit weight of the grout; and μ_g is the grout viscosity, which is a function of time t_{i-1}, the time required to inject up to $(i\text{-}1)^{th}$ shell. Eq. (4) can be used to calculate the time required for the grout to pass through a shell of width Δr. It is noteworthy that the time interval displayed in Eq. (4) can be expressed in a more general form as follows by combining Eqs. (1)-(2) and incorporating time step

$$\Delta t_{i,j} = \frac{Q_{j,j} \cdot n_0}{\gamma_g \cdot (K_{int})_{i,j} \cdot i \cdot A_{i,j}}(\mu_g)_{i,j} \tag{5}$$

where the subscripts i and j denote the sequence of radial spaces and time step, respectively, and i is $\leq j$. n_0 is the initial porosity of the ground, $Q_{j,j}$ is the last shell volume (between $j\text{-}1$ and j) at time step j (i.e., $i = j$), $(\mu_g)_{i,j}$ is the grout viscosity between r_{i-1} and r_i at time step j, and $(K_{int})_{i,j}$ is the intrinsic permeability coefficient between r_{i-1} and r_i at time step j.

2.2 Proposed method

In this study, Eq. (5) is modified for use in the development of a real time grouting monitoring system that can reflect the variations of injection pressure in real time. The shell volume between r_{i-1} and r_i at time step j can be expressed as follows

$$Q_{i,j} = \frac{\Delta t \cdot \gamma_g \cdot (K_{int})_{i,j} \cdot i \cdot A_{i,j}}{n_0 \cdot (\mu_g)_{i,j}} \tag{6}$$

where Δt is unit time (1 sec), i is the hydraulic gradient calculated from the injection pressure measured in real time when passing through r_{i-1} and r_i at time step j. The hydraulic gradient, i can be obtained by

$$i = \frac{P_{measured}}{\gamma_w \cdot \sum_0^{j-1}\Delta r_i} \tag{7}$$

where $P_{measured}$ is the measured injection pressure, γ_w is the unit weight of water, $\sum_0^{j-1}\Delta r_i$ is the penetration distance until time step $j\text{-}1$, and Δr_i is the penetration distance per unit time ($=\Delta t$), illustrated in Fig. 2.

To estimate Δr_i, the injected flow volume per unit time is to be calculated first. The shells of thickness Δr_i are placed consecutively, and then, the flow volume through each shell is ensured to be equal. Accordingly, the smallest injection volume among the calculated injection volumes that can pass through each shell in unit time governs the system. The last shell volume at time step j can be obtained as follows

$$Q_{j,j} = \min\left(Q_{0,j}, Q_{1,j}, Q_{2,j}, Q_{3,j} \cdots Q_{j,j}\right) \tag{8}$$

The fluid volume passing through the shell between r_{i-1} and r_i at time step j (Q_j) could be obtained as follows

$$Q_j = Q_{j,j} \cdot n_0 \tag{9}$$

From the above equation, the total penetration distances at times $j\text{-}1$ and j are obtained; these distances are expressed by Eqs. (10) and (11), respectively

$$r_{i-1} = \sqrt[3]{\frac{3}{4\pi}\sum_{j=0}^{i-1} Q_{j,j}} \tag{10}$$

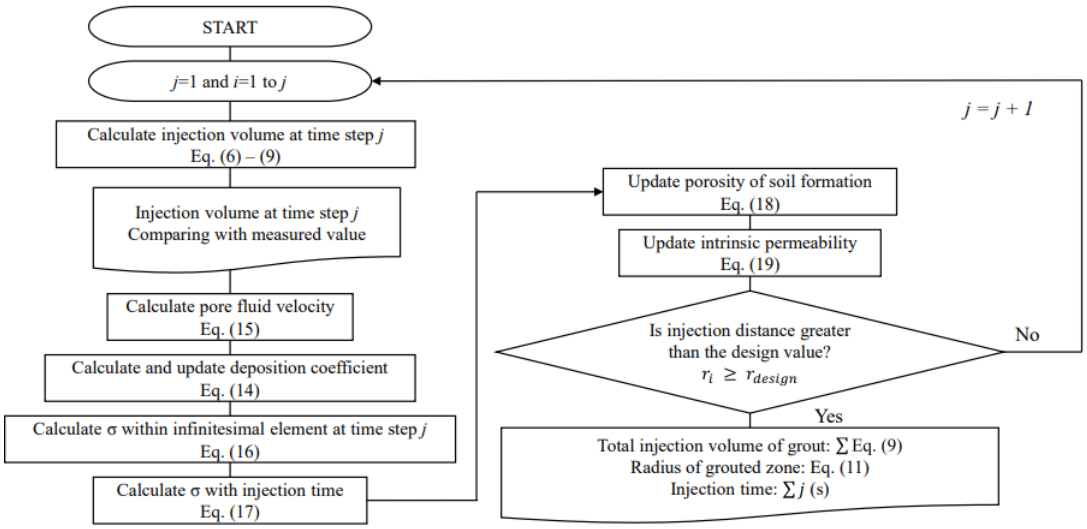

Fig. 3 Algorithm of real time grouting management system

$$r_i = \sqrt[3]{\frac{3}{4\pi}\sum_{j=0}^{i} Q_{j,j}} \tag{11}$$

Then, Δr_i can be obtained by subtracting Eq. (10) from Eq. (11)

$$\Delta r_i = r_i - r_{i-1} \tag{12}$$

The injection volume per unit time, Q_j, obtained from Eq. (9) is also referred to as the flow rate and is the core parameter to be obtained using the real time grouting management system presented in this paper. Predicted Q_j values are compared with flow rate values ($Q_{measured}$) measured in real time to assess the grouting injection status.

2.3 Clogging theory

Clogging phenomenon that occurs in the pores of the ground is to be considered in a real time grouting management system; it reduces the porosity of the ground during grout injection and eventually results in decrease of the permeability coefficient. In permeation grouting that uses cement with a high w/c ratio as a grout material and does not use cement-based accelerator, the variation in viscosity with time is not significant, and the groutability is largely regulated by the clogging phenomenon.

Adsorption and/or deposition of grout particles in pores in saturated ground was studied by Ives (1982), Payatakes *et al.* (1980), and Gruesbeck and Collins (1982). Finally, Kim *et al.* (2009) summarized the deposition model of grout particles. Deposition amount in soil pores can be expressed as follows

$$\sigma(r,t) = \int \lambda_{i,j} \cdot c_0 \cdot \frac{(r_0)^2}{\exp\left[-\frac{\lambda}{v_{i,j}} \cdot r_0\right] \cdot r^2} \cdot \exp\left[-\frac{\lambda}{v_{i,j}} \cdot r\right] \cdot \left(t - \frac{r}{v_{i,j}}\right) \tag{13}$$

where σ is the mass of the deposited particles per unit pore volume, r is the radial distance of an arbitrary point from the injection hole, r_0 is the radius of the injection hole, t is an arbitrary point in time, $\lambda_{i,j}$ is the deposition coefficient, $v_{i,j}$ is the radial pore velocity, and c_0 is the initial concentration of the grout. The parameter $\lambda_{i,j}$ is a function of the pore velocity and is expressed as follows (Reddi *et al.* 1997)

$$\lambda_{i,j} = \frac{v_{i,j}}{\alpha^* \cdot e^{2(b^2+m)}}\left[4(a\cdot\theta)^2 - 4(a\cdot\theta)^3 \cdot e^{(b^2-2m)/2} + (a\cdot\theta)^4 e^{2(b^2-m)}\right] \tag{14}$$

where m is the logarithmic mean of the pore radii, b is the logarithmic standard deviation of the pore radii, a is the radius of the grout particle, α^* is the effective length of the pore tube (α^*= 0.911 cm, suggested by Arya and Dierolf (1989)), and θ is a lumped parameter that takes into account the effect on deposition of several interparticle forces such as gravitational, inertial, hydrodynamic, electric double layer, and van der Waals forces. All the parameters in Eq. (14) apart from the pore velocity ($v_{i,j}$) are related to either the ground or grout. Based on Eq. (9), the pore velocity can be expressed as follows

$$v_{i,j} = \frac{Q_{j,j} \cdot n_0}{\Delta t \cdot A_{i,j} \cdot n_{i,j}} \tag{15}$$

Substituting Eqs. (14) and (15) in Eq. (13), the deposited amount at r_i at a unit time Δt can be expressed as follows

$$\Delta\overline{\sigma}_{i,j} = \sigma\left(r_i - \frac{\Delta r_i}{2}, \Delta t\right) \tag{16}$$

Then, the total deposited amount can be obtained by summation of Eq. (16) as follows

$$\sigma_{i,j} = \sum_{n=i}^{j} \Delta\overline{\sigma}_{i,n} \tag{17}$$

where $\sigma_{i,j}$ is the mass of the grout deposited into the pores until time step j. The porosity at time step j+1 can then be deduced as follows

$$n_{i,j+1} = n_0 - \frac{\sigma_{i,j}}{G_g \cdot \gamma_w} \tag{18}$$

Table 1 Criteria for assessing the grout penetration status

Flow rate	Injection pressure	Status
$Q_{measured} \fallingdotseq Q_{predicted}$	increasing tendency	adequately injected
$Q_{measured} < Q_{predicted}$	increasing tendency	adequately injected; however, likely to be influenced by heterogeneity of the ground
$Q_{measured} > Q_{predicted}$	decreasing tendency	fracturing occurs

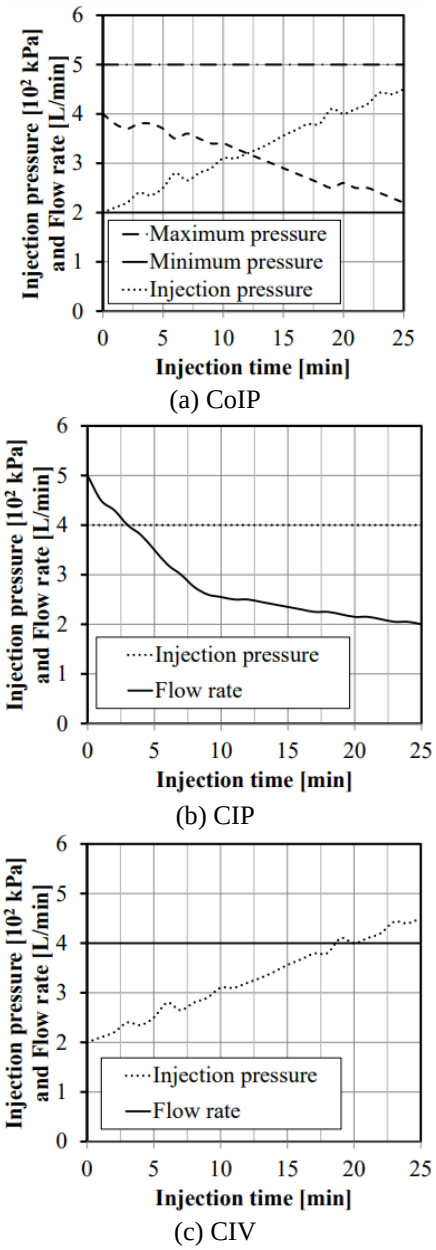

(a) CoIP

(b) CIP

(c) CIV

Fig. 4 Examples of three grout injection methods

where n_0 is the initial porosity, and G_g is the specific gravity of the grout. The permeability coefficient at time step j+1 can then be updated using the updated value of the porosity based on the Kozeny-Carman equation, as follows

$$(K_{int})_{i,j+1} = (K_{int})_{i,j} \cdot \frac{(1-n_{i,j})^2}{(n_{i,j})^3} \cdot \frac{(n_{i,j+1})^3}{(1-n_{i,j+1})^2} \quad (19)$$

Then, the shell volume that can pass through r_{i-1} and r_i at time step j+1 can be estimated by applying the updated porosity and permeability coefficient as follows

$$Q_{i,j+1} = \frac{\Delta t \cdot \gamma_g \cdot (K_{int})_{i,j+1} \cdot i \cdot A_{i,j}}{n_0 \cdot (\mu_g)_{i,j+1}} \quad (20)$$

The algorithm of the real time grouting management system based on clogging theory is illustrated in Fig. 3. The algorithm specifies the procedure for calculating the injection volume using updated values of porosity and permeability coefficient which vary as a result of clogging phenomenon. Then, it is feasible to assess the effectiveness of the injection work by comparing the injection volume calculated using the algorithm with that measured in real time. Finally, when the penetration distance exceeds the designed value, injection could be stopped.

2.4 Main features of the proposed system

Comparing with currently available systems, the most distinguished feature of the proposed system is that injection pressure measured in real time was used as an input variable. It implies that the prediction results are influenced by changing ground condition and injection status in real time. The main features of the proposed system are presented as follows.

2.4.1 Estimation of flow rate and penetration distance in real time

The injection volume per unit time can be estimated using Eq. (9). It was feasible to assess the injection status in real time by comparing the estimated injection volume per unit time with the flow rate measured during the grout injection. The criteria for assessment are presented in Table 1.

The penetration distance of the grout can also be estimated in real time from Eq. (11). If the penetration distance attains the designed value, it can serve as the stop criteria.

2.4.2 Injection pressure estimation in real time

Grout injection methods can be classified as constant injection pressure (CIP) method, constant injection volume (CIV) method, and controlled injection pressure (CoIP) method (please see Fig. 4). While constant values of pressure or volume are maintained all through till the end in the constant injection pressure method or the constant injection volume method, respectively, in the controlled injection pressure method, the injection pressure is always regulated such that it ranges between P_{min} and P_{max}; here, P_{min} is the minimum pressure that enables grout penetration, and P_{max} is the upper bound pressure required for preventing fracture. These bound values are obtained in advance from preliminary test using water as a fluid. The main drawback of the constant injection volume method is that as constant flow rate is applied all through, it is not feasible to identify and prevent fracturing of the ground during grout injection in the field. Therefore, controlled injection pressure (CoIP) method is generally adopted in practice in case of permeation grouting.

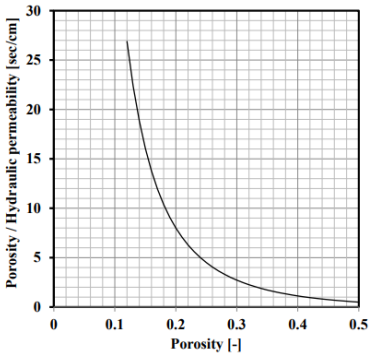

Fig. 5 Porosity/Permeability Coefficient vs. Porosity (n_0 = 0.5, K_0 = 1 cm/s, $\mu_g(0)$ = 1 mPa·s)

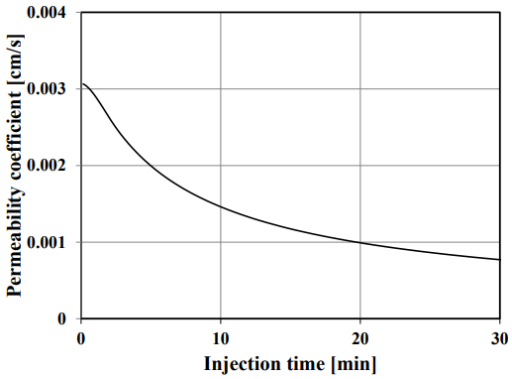

Fig. 6 Example of permeability coefficient variation in real time (K_0 = 3.38 × 10^{-3} cm/s, designed grouting radius = 50 cm)

Accordingly, in this study, the CoIP model, which is generally used for permeation grouting, is adopted. The present authors intend to predict the grouting status at a designated time by estimating the flow rate as well as the injection pressure. The methodology for estimating the injection volume was adequately explained in sections 2.2 and 2.3; this section describes the methodology for predicting injection pressure.

In order to estimate the injection pressure, it is necessary to estimate the hydraulic gradient. From Eq. (4), the hydraulic gradient can be expressed as

$$i_{i,j} = \frac{\Delta r_{i,j} \cdot n_{i,j}}{\gamma_g \cdot (K_{int})_{i,j} \cdot \Delta t_{i,j}} \mu_g(t_{i-1}) \tag{21}$$

According to Eq. (21), the hydraulic gradient is proportional to the viscosity of the grout and porosity, and inversely proportional to the permeability coefficient. Fig. 5 plots the results of the parametric study, wherein the value of $n_{i,j}/(K_{int})_{i,j}$, (see Eq. (21)) is compared with the porosity value. Although both the permeability coefficient and porosity decrease owing to clogging phenomenon during grout injection, Fig. 5 clearly illustrates that the decreasing tendency of the permeability coefficient is more significant than that of the porosity; it implies that the hydraulic gradient increases with time, mainly because of the clogging phenomenon.

The reduction in pressure at a designated time and location can be estimated as follows by using the hydraulic gradient obtained in Eq. (21)

$$\Delta p_{i,j} = i_{i,j} \cdot \gamma_w \cdot \Delta r_i \tag{22}$$

Eq. (22) is used to calculate the reduced pressure as the grout passes through a shell Δr_i; this implies that this parameter is the pressure reduction in one shell; the pressure reduction when the grout passes through the entire area up to the time step j is expressed as follows

$$\Delta p_j = \sum_{i=0}^{j} i_{i,j} \cdot \gamma_w \cdot \Delta r_i \tag{23}$$

In order to ensure grout penetration into an additional shell, an injection pressure higher than that calculated by Eq. (23) is required, and the equation used to predict the injection pressure at time step j+1 is as follows

$$\Delta p_{predicted}{}_{j+1} = \Delta p_j + \Delta p_{j+1,j+1} \tag{24}$$

To obtain the pressure required for injection into the $(i+1)^{th}$ shell ($\Delta P_{j+1,j+1}$), the injection volume per unit time as well as the $\Delta r_{j+1,j+1}$ value is to be determined in advance. However, as the injection pressure as well as injection volume per unit time varies with time in the CoIP model, it is not feasible to determine the value of $\Delta r_{j+1,j+1}$ in advance; i.e., it is necessary to assume the injection volume per unit time and use trial-and-error method to obtain the value of $\Delta r_{j+1,j+1}$. This method will be explained in detail in Chapter 4 using actual measured data at job sites.

2.4.3 Permeability coefficient estimation in real time

The most critical feature of the proposed system, which distinguishes it from existing grouting management systems, is that it is capable of estimating the permeability coefficient at any location in real time. In general, a requirement for additional injection is identified by measuring the permeability coefficient after the completion of initial injection and comparing this value with the initial value. However, if the permeability coefficient could be estimated in real time, a number of additional injections could be averted by terminating the injection when the estimated permeability coefficient attains the designed value. An example of analysis result of permeability coefficient with elapse of time, estimated using the proposed algorithm, is illustrated in Fig. 6.

3. Fracturing and fractured volume estimation

Ground fracturing phenomena which involve the creation of a fracture and injection through this fracture can occur without warning during grouting work even in permeation grouting; this is mainly owing to the heterogeneity of the ground. In such a case, injected grout material is mostly used to fill the fractured gap rather than for permeation through the ground. Wang *et al.* (2016) reported in their study that compaction grouting is dominant in low pressure grouting irrespective of the w/c ratio, and, in high pressure grouting, the likelihood of a fracture occurrence increases with the increase of the w/c ratio. Yun *et al.* (2016) also theoretically and experimentally

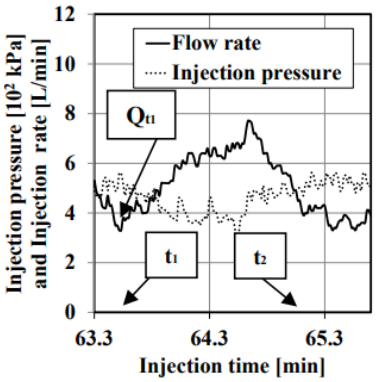

Fig. 7 Occurrence of fracture during permeation grouting

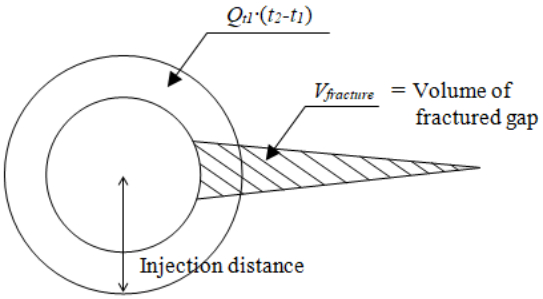

Fig. 8 Conceptual diagram of the shape of the fractured gap

established that a fracture is likely to occur when the injection pressure exceeds 120% of the overburden pressure; they presented an equation for estimating the length and thickness of the fractured gap. These two studies established that the likelihood of occurrence of a fracture increases when grout material with high w/c ratio is used.

In general, if ground fracturing occurs during grout injection, the injection pressure drops temporarily with the opening of a new gap in the ground, and the injection volume abruptly increases to fill the crack. The present authors investigated the relationship between the pressure reduction and fracture gap volume by utilizing the field data from two grouting job sites; 13 injection holes were analyzed to formulate the relationship between the two parameters.

3.1 Define pressure reduction and injection volume for fracture

A majority of injection equipment contains a pressure pump, and owing to its characteristics, pulsation and/or fluctuation in injection pressure always occur. Regardless of this fluctuation, occurrence of fracture during the grout injection can be predicted effectively by observing the injection pressure and flow rate in real time. If the injection pressure drops significantly (significantly exceeding the regular pressure fluctuation) along with the abrupt increase of the flow rate, the occurrence of fractures can be conveniently notified. For example, the decrease of the injection pressure as well as increase of the flow rate at time t_1 can be observed in Fig. 7; a fracture initiates at t_1, and the flow rate increase significantly to fill the fractured gap until time t_2, when the reduced injection pressure is recovered.

It can be observed that the injection pressure (dotted line) has decreased at approximately t_1 and recovered at t_2; the variation between the maximum and minimum values of the injection pressure between t_1 and t_2 is defined as the pressure reduction. The volume of the fractured gap, as illustrated in the schematic in Fig. 8, can be obtained by the following

$$V_{fracture} = \int_{t_1}^{t_2} Q_{measured} - Q_{t_1} \cdot (t_2 - t_1) \qquad (25)$$

where $V_{fracture}$ is the volume of the fractured gap to be filled in by the grout (defined as the injection volume for fracture), t_1 is the time at which the pressure starts to decrease, t_2 is the time at which the pressure is completely recovered, $Q_{measured}$ is the measured flow rate, and Q_{t1} is the flow rate at t_1.

3.2 Relationship between pressure reduction and injection volume for fracture

Grout monitoring data were collected from the two job sites, K site and D site, where permeation grouting works were conducted to minimize the water leakage near a reservoir. The ground conditions of the two sites are presented in Fig. 9. Weathered soil is in the upper layer, and weathered rock and/or soft rock ground is distributed in the lower layers. The grouting work was carried out for the weathered soil layer, and the permeability coefficients of the weathered soil in both of the sites are in the range 10^{-4}–10^{-3} cm/s.

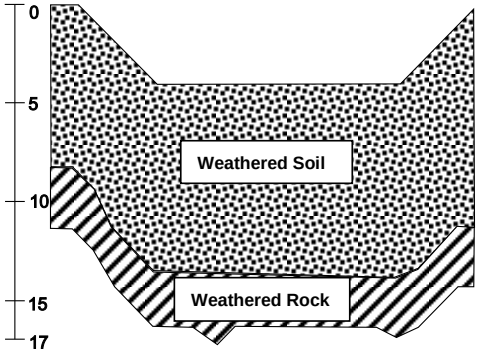

(a) K site

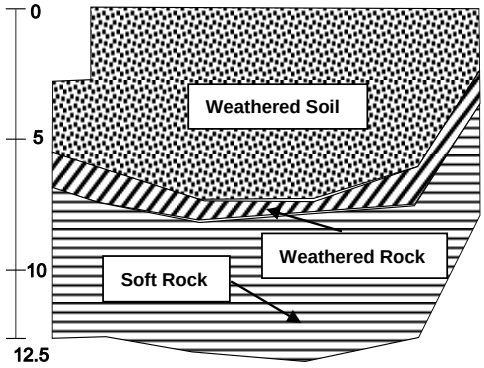

(b) D site

Fig. 9 Geological conditions of the sites

Table 2 Pressure reduction and injection volume for each fracture

Site	Pressure reduction [kPa]	Injection volume for fracture [cm^3]	Pressure reduction [kPa]	Injection volume for fracture [cm^3]
K site	150	1,428	240	3,016
	150	1,703	260	2,561
	220	3,150	-	-
D site	40	258	30	788
	40	72	150	2,502
	130	1,051	80	838
	70	1,028	60	1,021

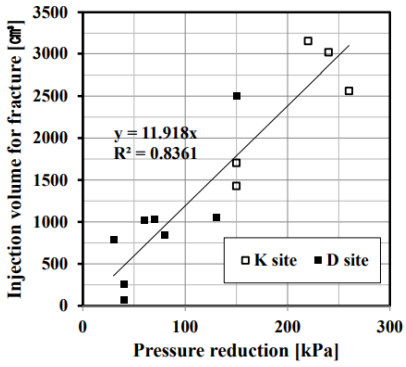

Fig. 10 Relationship between pressure reduction and injection volume for fracture

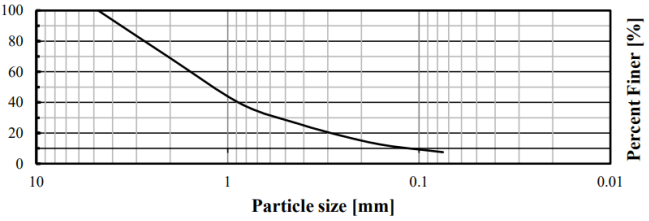

Fig. 11 Particle size distribution curve (K site)

Table 3 Soil properties of weathered granite soil at K site

Weathered Granite soil	
Specific gravity [-]	2.60
Unit weight [kN/m^3]	17.7
Friction angle [°]	32.74
Cohesion [kPa]	20.47
Permeability coefficient [cm/sec]	1.195 × 10-3

By analyzing the monitoring data, the occurrence of fractures was identified at seven locations and/or times; the pressure reduction and injection volume for fracture was obtained at each fracture; the results are summarized in Table 2.

The relationship between the measured pressure reduction and injection volume to fill the fractured gap is plotted in Fig. 10 using the data presented in Table 2. Fig. 10 illustrates that the two variables exhibit a proportional linear relationship, and the correlation coefficient was significantly high (0.83). Then, an empirical formula was proposed in this study as follows

$$V_{fractured}\,(cm^3) = 11.918 \cdot \Delta p\,(kPa) \quad (26)$$

where Δp is the pressure reduction. Using Eq. (26), it is feasible to estimate the volume of the grout that is required to fill the fractured gap in the event that fracture occurs during the permeation grouting work.

4. A case study

4.1 Input parameters

The grouting management system proposed in this study was analyzed and verified using the monitoring data gathered from the K site among the two job sites mentioned above. The particle size distribution curve and soil properties of K site are illustrated in Fig. 11 and summarized in Table 3, respectively.

Input parameters of the weathered granite soil at K site as well as those of the grout material are summarized in Table 4.

Monitoring data were collected at weathered granite soil layer with 7-10 m depth; at both the sites, the granite soil layers are located below the groundwater level and are completely saturated. The w/c ratio of the grout was 1.3, and grout work was conducted without using hardening accelerator. The permeability coefficient presented in Table 4 is significantly higher than the average permeability coefficient of general weathered granite soil, ≈ 10^{-6}–10^{-5} cm/s. As the site has been in a condition wherein extensive leakage of groundwater has occurred and a flow channel is formed, the permeability coefficient was as high as 1.195 × 10^{-3} cm/s.

The measured injection pressure and flow rate data monitored during grout injection are presented in Fig. 12. Except for the instant of fracture occurrence, the flow rate decreases, and the injection pressure exhibits an increasing trend with time as illustrated in Fig. 12.

Table 4 Input parameters of ground and grout (K site)

Ground parameters		Grout parameters	
m [-]	-2.306	c_0 [g/cm^3]	1.2
b [-]	1.410	γ_g [t/m^3]	1.255
K [cm/s]	1.195 × 10^{-3}	G_g [-]	3.0
n [-]	0.3	$\mu_g(t)$ [10^{-3} Pa·s]	0.00094 × t^2 + 0.142 × t + 58.97
θ [-]	6.5	a [mm]	0.011

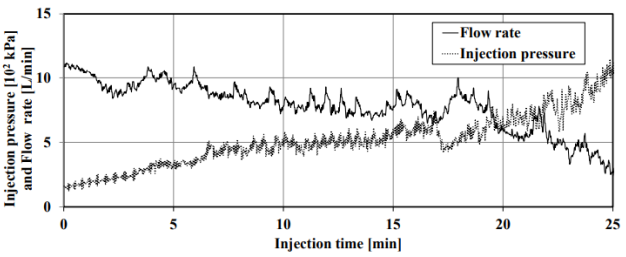

Fig. 12 Grout monitoring data measured in real time (K site)

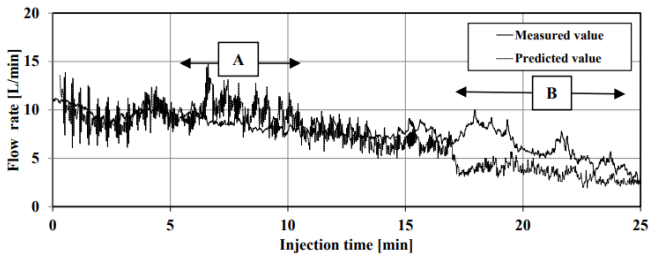

(a) Analysis result considering clogging phenomenon

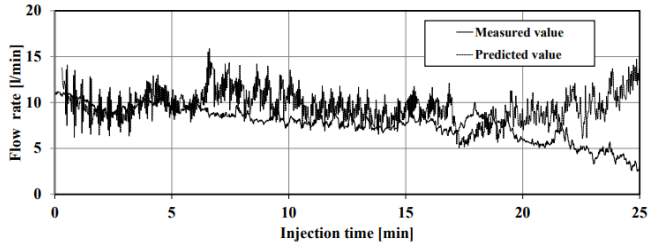

(b) Analysis result without considering clogging phenomenon

Fig. 13 Comparison of flow rate predicted by the proposed system with measured flow rates

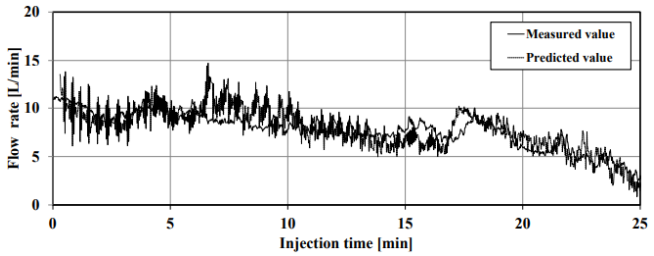

Fig. 14 Flow rate estimation taking into account injection volume for fracture

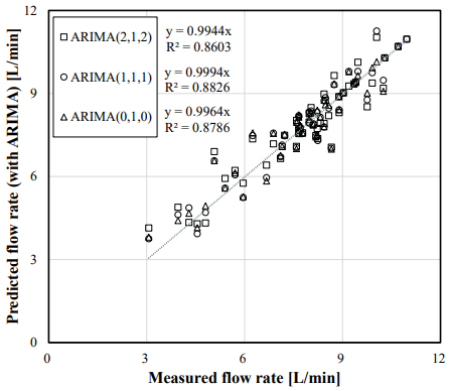

Fig. 15 Comparison results and coefficients of determination

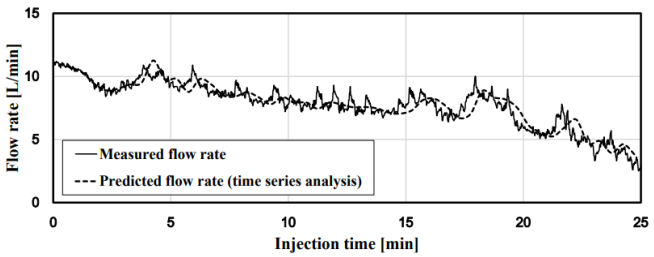

Fig. 16 Flow rates predicted using the ARIMA (1,1,1) model

4.2 Flow rate estimation

The flow rate was predicted utilizing the proposed system and using the injection pressure as the input data; then, the predicted value was compared with the measured one presented in Fig. 13(a). Because of fluctuation of the measured injection pressure (which was used as the input data), the predicted flow rate also exhibited fluctuations compared to the measured one; however, the two curves matched reasonably well except at two instants, at sections A and B (see Fig. 13(a)).

The sections where the predicted values and measured values varied significantly were the following:

• Section A: Here, the pressure exhibits a continuously increasing trend (see Fig. 12) in the relevant section, and the predicted flow rate is larger than the measured flow rate. As defined in Table 1, in this case, the ground condition in Section A may have higher density and lower porosity than other areas owing to heterogeneity of the ground.

• Section B: Here, the pressure decreases, and the predicted flow rate and measured flow rate display opposite trends. It can be seen that the prediction accuracy slightly decreased due to occurrence of small fractures at around 15 min. From Table 1, it can be observed that a large fracture has occurred in the ground and that several fractures have occurred continuously after a large fracture occurred at approximately 17 min.

Section B of Fig. 13(a) was modified to take into account the increase of the injection volume for fracture based on Eq. (26); the modified curves are illustrated in Fig. 14. It can be observed that consistency between the two curves is high with the inclusion of additional injection volume to fill the fractured gap.

As mentioned in section 2.3, the main characteristics of the proposed real time grouting management system is that the clogging phenomenon is taken into account. For comparison, the flow rate is predicted without considering the clogging phenomenon, and the results are illustrated In Fig. 13(b). Fig. 13(b) clearly demonstrates that the deviation between the predicted and measured value is significant; it is not capable of predicting the decreasing tendency of the flow rate as the clogging effect was not taken into consideration.

4.3 Injection pressure estimation

As mentioned earlier in Chapter 2, when the CoIP model is adopted to predict the injection pressure at a location for a designated period of time, it is essential to assume the injection volume per unit time in advance. In the present study, it is proposed to predict the injection volume per unit time by utilizing a time series analysis technique (Montgomery *et al.* 2015).

Among the various time series model, such as moving average (MA) model, auto regressive (AR) model, ARMA model, ARIMA model etc., the ARIMA model is chosen in this study taking the non-stationarity of the grout monitoring data measured in real time as shown in Fig. 12. The flow rate monitoring data shown in Fig. 12 was analyzed utilizing the IBM SPSS Statistics 24.0 (IBM Corp. 2016) to determine the optimal ARIMA model. The

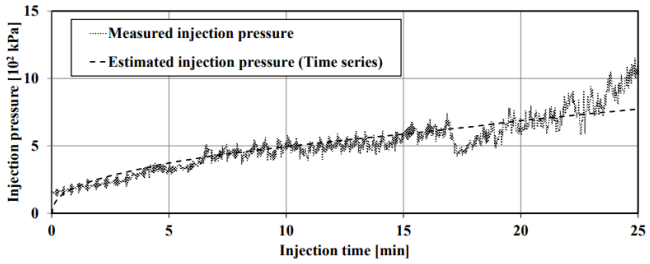

Fig. 17 Injection pressure prediction results

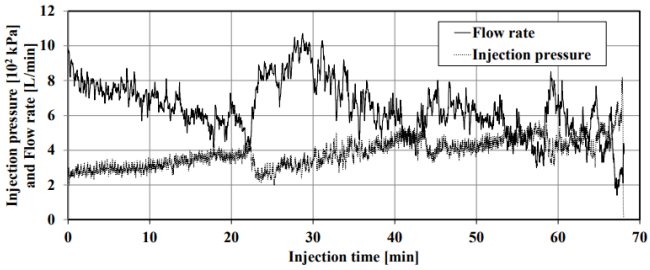

Fig. 18 Monitoring data with multiple fractured injection incidents

Table 5 Additional injection volume to fill the fractured gap

Time [min]	Additional injection volume for fracture [L]
22.2–41.5	121.59
43.8–45.7	3.8
58.3–62.5	18.9
63.5–65.4	7.22
65.6–66.8	3.6
Total	155.11

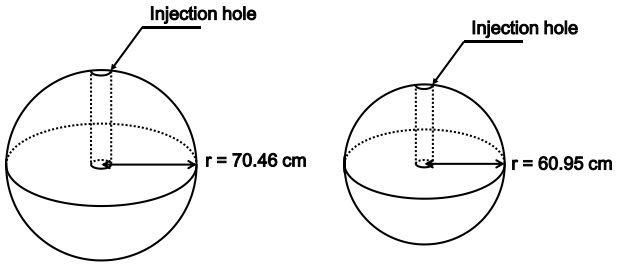

(a) Fracturing phenomenon not taken into account (b) Fracturing phenomenon taken into account

Fig. 19 Grout bulb radius depending on fracture consideration

analysis results are summarized in Fig. 15. From these results, the most optimal time series model to predict the flow rate in real time is determined to be ARIMA (1,1,1); for details of this model please see Montgomery *et al.* (2015). The flow rates with time are back-predicted again using the ARIMA (1,1,1) model proposed in this study and are shown in Fig. 16 along with the monitored results in real time. Fig. 16 shows that the two curves match reasonably well indicating the validity of the proposed ARIMA (1,1,1) model.

Then, the injection pressures with time were predicted using Eqs. (20)-(24) by inputting the flow rates that were predicted utilizing the ARIMA (1,1,1) model; the predicted result are plotted in Fig. 17 along with those measured in real time. The figure illustrates that the predicted injection pressure and measured injection pressure matches reasonably well. This indicated that the grout injection at the job site was functioning adequately with no anomalies in the ground, and it also verified that the method of predicting the injection pressure by utilizing the time series analysis technique is also valid. The predicted result of the injection pressure illustrated in Fig. 17 can be used to predict the feasibility of ground fractures by comparing the predicted injection pressure to the critical injection pressure (P_{max} value) during grouting work. Pre-determined P_{max} value obtained from the preliminary test using water as a fluid was 5 bar; a fracture is highly likely to occur when P_{max} increases above this value. Fig. 17 illustrates that occurrence of fracture is feasible at 10 min or beyond from the start of the injection; moreover, it can be observed that a fracture actually occurred 17 min after the injection started.

4.4 Injected bulb radius (penetration distance) estimation

In the case of spherical penetration, the volume of the injected grout bulb can be obtained by integrating the injected flow rate over the whole injection period. If the main purpose of the grouting is to increase the strength of the ground, this can be achieved by stiffening the ground notwithstanding the occurrence of fractures during permeation grouting. However, if the main purpose is water cutoff rather than strengthening the ground, the radius of the grout bulb penetrated into the ground (penetration distance) is even more critical in assessing the quality of the grouting work. If the diameter of the grout bulb is significantly decreased owing to frequent occurrence of fractures, the radius of the grout bulb is likely to be inadequate to form a cutoff wall.

Fig. 18 depicts a case history where numerous fractured injection incidents have occurred during grouting work at the same job site. In such a case, if the grout bulb is straightforwardly calculated using only the injected volume of the grout, it is overestimated. The injection volumes to fill the fractured gaps were calculated using Eq. (25) and are summarized in Table 5; the radius of the spherical penetration considering the effect of the fractures is presented in Fig. 19(b) for comparison with that presented in Fig. 19(a), in which the radius was calculated without taking into account the effect of the occurrence of fractures.

The total injection volume obtained by integrating the measured flow rate over the entire injection time was 439.6 L (with the radius of 70.46 cm); however, this volume includes the volume to fill the fractured gaps as well as that consumed to penetrate the ground. The calculated injection volume to fill the fracture gaps was 155.11 L, and the calculated bulb radius excluding it was 60.95 cm. From this, it can be observed that the radius of the grout bulb formed as a result of permeation grouting decreases by approximately 10 cm when the fracturing phenomenon is taken into account. In other words, if the fracturing phenomenon is not taken into account, the volume of the

grout bulb can be overestimated.

5. Conclusions

In this study, the authors have proposed a real time grouting management system based on clogging theory. The new system measures the injection pressure in real time; then, the flow rate with elapse of time can be predicted using the measured injection pressure. By comparing the predicted flow rate with the measured one in-situ, quality of the grouting work can be adequately monitored and managed in real time. The summary and limitations of this study are as follows:

• Although cement-based permeation grouting for soils with high w/c ratio is affected by numerous factors, it has been verified through application of field data that the most critical factor is the clogging phenomenon occurring during grout injection.

• The adequacy of grouting work for soils can be assessed in real time by the proposed real time grouting management system, in which injection pressure and/or flow rate are estimated based on the clogging theory and compared with monitored data.

• The possibility of occurrence of fractures can be predicted conveniently using the proposed system by predicting the injection pressure using the time series analysis technique.

• The volume of the grout bulb can be estimated more accurately by taking into account the volumetric loss of the grout bulb caused by the occurrence of fracture. The radius of the formed grout bulb then can be calculated more accurately.

• In this study, the investigation was conducted with limited conditions of permeation grouting using cement milk (Newtonian fluid) with a high w/c ratio, into saturated ground. In future, further studies are required on grouting using a Bingham fluid and/or a power-law fluid with a low w/c ratio; furthermore, a study of grouting phenomenon penetrating through unsaturated ground is also required.

Acknowledgements

This research was supported by a grant (Project number: 16SCIP-B066321-04 (Development of Key Subsea Tunnelling Technology)) from Infrastructure and Transportation Technology Promotion Research Program funded by Ministry of Land, Infrastructure and Transport of the Korean government.

References

Arya, L.M. and Dierolf, T.S. (1989), "Predicting soil moisture characteristics from particle-size distributions: An improved method to calculate pore radii from particle radii", *Proceedings of the International Workshop on Indirect Methods for Estimating the Hydraulic Properties of Unsaturated Soils*, University of California, Riverside, California, U.S.A.

Axelsson, M., Gustafson, G. and Fransson, A. (2009), "Stop mechanism for cementitious grouts at different water-to-cement ratios", *Tunn. Undergr. Sp. Technol.*, **24**(4), 390-397.

Do, J., Park, J., Choi, D. and Chun, B. (2012), "A study on the field application of automatic grouting system", *J. Kor. Geoenviron. Soc.*, **13**(1), 63-74.

Fan, G., Zhong, D., Ren, B., Cui, B., Li, X. and Yue, P. (2016), "Real-time grouting monitoring and visualization analysis system for dam foundation curtain grouting", *Trans. Tianjin University*, **22**(6), 493-501.

Gruesbeck, C. and Collins, R.E. (1982), "Entrainment and deposition of fine particles in porous media", *J. Soc. Petroleum Engineers*, **22**(6), 847-856.

IBM Corp. (2016), *IBM SPSS Statistics for Windows*, Version 24.0. Armonk, New York, U.S.A.

Ives, K.J. (1982), "Fundamentals of filtration", *Proceedings of the 21st European Federation of Chemical Engineering Event Symposium on Water Filtration*, Antwerp, Belgium.

Kim, J.S., Lee, I.M., Jang, J.H. and Choi, H. (2009), "Groutability of cement-based grout with consideration of viscosity and filtration phenomenon", *J. Numer. Anal. Mech. Geomech.*, **33**(16), 1771-1797.

Kobayashi, S., Stille, H., Gustafson, G. and Stille, B. (2008), *Real Time Grouting Control Method. Development and Application using Aespoe HRL Data*, No. SKB-R-08-133, Swedish Nuclear Fuel and Waste Management Co.

Montgomery, D.C., Jennings, C.L. and Kulahci, M. (2015). *Introduction to Time Series Analysis and Forecasting*, 2nd edition, John Wiley & Sons, Inc., Hoboken, New Jersey, U.S.A.

Payatakes, A.C., Ng, K.M. and Flumerfeit, R.W. (1980), "Oil ganglion dynamics during immiscible displacement: Model formulation", *J. ALChE*, **26**(3), 430-443.

Raffle, J.F. and Greenwood, D.A. (1961), "The relationship between the rheological characteristics of grouts and their capacity to permeate soils", *Proceedings of the 5th International Conference on Soil Mechanics and Foundation Engineering*, Paris, France, July.

Reddi, L.N. and Bonala, M.V. (1997), "Analytical solution for fine particle accumulation in soil filters", *J. Geotech. Geoinviron. Eng.*, **123**(12), 1143-1152.

Taylor, R.M. and Choquet, P. (2012), "Automatic monitoring of grouting performance parameters", *Proceedings of the 4th International Conference on Grouting and Deep Mixing*, New Orleans, Louisiana, U.S.A., February.

Wang, Q., Wang, S., Sloan, S.W., Sheng, D. and Pakzad, R. (2016), "Experimental investigation of pressure grouting in sand", *Soils Found.*, **56**(2), 161-173.

Yang, Z.Q., Hou, K.P. and Guo, T.T. (2011), "Study on the effects of different water-cement ratios on the flow pattern properties of cement grouts", *Appl. Mech. Mater.*, **71**, 1264-1267.

Yun, J.W., Park, J.J., Kwon, Y.S., Kim, B.K, and Lee, I.M. (2017), "Cement-based fracture grouting phenomenon of weathered granite soil", *KSCE J. Civ. Eng.*, **21**(1), 232-242.

GC